Correlated Emission Lasing in Harmonic Oscillators Coupled via a Single Three-Level Artificial Atom

Z. H. Peng,[1,2,*] Yu-xi Liu,[3,4] J. T. Peltonen,[1] T. Yamamoto,[5] J. S. Tsai,[6,1] and O. Astafiev[2,1,7,8,†]

[1]*Center for Emergent Matter Science, RIKEN, Wako, Saitama 351-0198, Japan*
[2]*Physics Department, Royal Holloway, University of London, Egham, Surrey TW20 0EX, United Kingdom*
[3]*Institute of Microelectronics, Tsinghua University, Beijing 100084, China*
[4]*Tsinghua National Laboratory for Information Science and Technology (TNList), Beijing 100084, China*
[5]*NEC Smart Energy Research Laboratories, Tsukuba, Ibaraki 305-8501, Japan*
[6]*Department of Physics, Tokyo University of Science, Kagurazaka, Tokyo 162-8601, Japan*
[7]*National Physical Laboratory, Teddington, TW11 0LW, United Kingdom*
[8]*Moscow Institute of Physics and Technology, Dolgoprudny, 141700, Russia*
(Received 7 May 2015; revised manuscript received 22 July 2015; published 25 November 2015)

A single superconducting artificial atom can be used for coupling electromagnetic fields up to the single-photon level due to an easily achieved strong coupling regime. Bringing a pair of harmonic oscillators into resonance with the transitions of a three-level atom converts atomic spontaneous processes into correlated emission dynamics. We present the experimental demonstration of two-mode correlated emission lasing in harmonic oscillators coupled via a fully controllable three-level superconducting quantum system (artificial atom). The correlation of emissions with two different colors reveals itself as equally narrowed linewidths and quenching of their mutual phase diffusion. The mutual linewidth is more than 4 orders of magnitude narrower than the Schawlow-Townes limit. The interference between the different color lasing fields demonstrates that the two-mode fields are strongly correlated.

Excited free atoms relax to their ground states via incoherent spontaneous emission processes [1]. In an ensemble of three-level atoms—the fundamental objects of quantum optics—coupling of the lowest pair of levels to a harmonic oscillator leads to conventional lasing if incoherent relaxation from the second excited state to the first excited state creates population inversion. The situation is dramatically changed when both transitions of the atoms are coupled to independent oscillators: the spontaneous emission processes are replaced by coherent energy exchange and correlated dynamics between the oscillators, known as correlated emission lasing (CEL) [1–6]. The correlated dynamics reveals itself as a reduction in relative random phase-diffusion noise, resulting in the suppression of the mutual peak width below the Schawlow-Townes limit [7]. The suppression of phase-diffusion noise has been experimentally observed for two polarization modes in a HeNe laser [4–6]. However, the best result observed so far has been about 2.3% of the Schawlow-Townes limit for an ensemble of natural atoms [6]. Recently, the classical lasing effect has been reproduced on single atoms [8] or single superconducting quantum systems (artificial atoms) [9–11], in which strong coupling to circuit elements can be easily achieved [9–13]. In this Letter, we demonstrate the coherent dynamics of two harmonic modes with different frequencies in a transmission line resonator (TLR) coupled through a single three-level artificial atom. Oppositely to the ensemble of atoms with uncorrelated dephasing in different ones, the single atom allows us to ideally suppress

the phase diffusion. We demonstrate quenching of the mutual phase diffusion to the level better than 10^{-4}. The correlation between two lasing fields is displayed in the interference between them.

In addition, we point out that our system presents a fundamentally new circuit. In usual quantum electrodynamics, atoms are coupled through a resonator mode, however, the reversed circuit with linear oscillators coupled via transitions of a quantum system is very difficult, if not impossible, to realize with natural atoms, spins or quantum dots. Such a system presents a novel approach and allows us to demonstrate a series of qualitatively new phenomena of quantum optics.

As shown in Fig. 1(a), Fig. 1(b), and Fig. 1(c), the single three-level artificial atom with cyclic transitions [14] is based on a "tunable gap flux qubit" circuit [15,16] capacitively coupled to a multimode transmission line resonator. Such a coupling for the flux qubits has been realized in Ref. [17] and the transition matrix elements for the three-level system calculated in Ref. [18] are consistent with our experiment. The artificial atom is situated in the voltage antinode of the resonator. The transition frequencies (ω_{eg}, ω_{dg}, and ω_{de}) between the three lowest levels of the atom $|g\rangle$, $|e\rangle$, and $|d\rangle$ (the ground, first excited, and second excited states) are controlled by an external magnetic flux, reaching minimal ω_{eg} and ω_{dg} at half-integer flux quanta $\Phi_N = (N + \frac{1}{2})\Phi_0$ (where N is an integer). Compared with systems based on the conventional flux
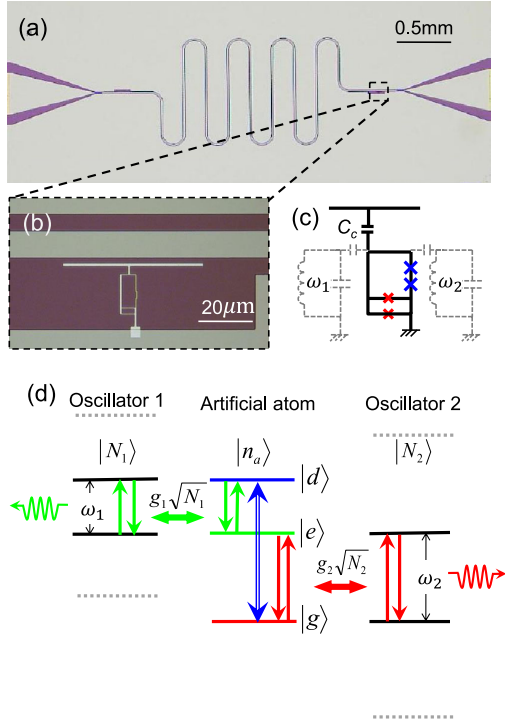
FIG. 1 (color online). Device description. (a) Optical micrograph of the device. The meandering structure is a TLR made of a 50-nm-thick Nb film capacitively coupled to external coplanar waveguides. (b) Magnified micrograph of an artificial atom based on the tunable gap superconducting flux qubit geometry. The α loop (with red junctions) allows the flux tunnelling energy to be tuned. (c) Simplified circuit model of the atom capacitively coupled to the TLR through capacitance C_c. The atom is effectively coupled to two oscillators with the frequencies ω_1 and ω_2, schematically shown by the dashed lines. (d) Principles of the device operation. The transitions $|d\rangle - |e\rangle$ and $|e\rangle - |g\rangle$ are resonant with the first and second oscillators, respectively. The transition $|g\rangle - |d\rangle$ is driven by a classical microwave pumping field.

qubit geometry [19,20], our atom has additional tunability owing to the implementation of an α loop—a dc SQUID, which allows the flux tunnelling energy Δ to be changed by choosing Φ_N. By selecting Φ_N and additionally tuning $\delta\Phi$ ($\ll \Phi_0$), one can adjust the transition frequencies ω_{eg} and ω_{de} to the resonance with the two lowest modes of the resonator—the two independent fixed-frequency oscillators r_1 and r_2 with the frequencies ω_1 and ω_2, respectively.

The entire system presented in Fig. 1(d) can be described by the state $|N_1 n N_2\rangle = |N_1\rangle \otimes |n\rangle \otimes |N_2\rangle$ with the three quantum numbers n, N_1, and N_2, denoting the three-level atomic states $|n\rangle = \{|g\rangle, |e\rangle, |d\rangle\}$ and the Fock states of resonators $|N_{1,2}\rangle = \{|0\rangle, |1\rangle, |2\rangle, \ldots\}$ with the photon occupation $N_{1,2}$ in the first and second oscillators. The full Hamiltonian of the two harmonic oscillators coupled via transitions of the three-level atom and driven by a microwave with the frequency $\omega_p \approx \omega_{dg}$ and amplitude $2\hbar\Omega$ is

$$H = \hbar\omega_1 a_1^\dagger a_1 + \hbar\omega_2 a_2^\dagger a_2 + \hbar\omega_{dg}\sigma_{dd} + \hbar\omega_{eg}\sigma_{ee}$$
$$+ \hbar g_1(a_1^\dagger \sigma_{ed} + a_1\sigma_{de}) + \hbar g_2(a_2^\dagger \sigma_{ge} + a_2\sigma_{eg})$$
$$+ 2\hbar\Omega(\sigma_{dg} + \sigma_{gd})\cos\omega_p t. \tag{1}$$

Here, $\sigma_{jk} = |j\rangle\langle k|$ is the projection or transition operator for the atomic states with $\{j, k\} = \{e, g, d\}$. $a_1^\dagger$ (a_1) and $a_2^\dagger$ (a_2) are the creation (annihilation) operators of the first and second oscillators, respectively. The atomic states $|g\rangle$ and $|d\rangle$ are coupled by the pumping field. To eliminate the time dependence, the Hamiltonian can be further simplified using the rotating wave approximation, in which the two oscillators appear to be resonantly coupled via the quantum system. The dissipative dynamics of this artificial atom-resonator coupled system is described by the Markovian master equation with taking energy relaxation and decoherence in the system into account [18].

We perform microwave characterization (transmission and emission measurements) of the device in a dilution refrigerator at a temperature of 30 mK. The device fabrication process and experimental setup are described in detail in the Supplemental Materials [18]. From the transmission measurement, $\omega_1/2\pi \approx 6.0016$ GHz and $\omega_2/2\pi \approx 11.9979$ GHz with the corresponding linewidths (decay rates) in the oscillators of $\kappa_1/2\pi = 0.63$ MHz and $\kappa_2/2\pi = 1.94$ MHz at the base temperature. We find that $\Phi_N \approx 1.5\Phi_0$ ($\Delta = h \times 1.51$ GHz) and $\delta\Phi \sim 18 \times 10^{-3}\Phi_0$ is one of the best choices to reach the desired double resonance. To characterize the atom-resonator interaction, we measure the normalized transmission through the system $|t/t_0|$ around ω_1 and ω_2 as a function of the probing frequency and flux bias $\delta\Phi$ using a vector network analyzer [Fig. 2(a) and Fig. 2(b)], where t_0 is the maximal transmission amplitude. Anticrossings due to vacuum Rabi splittings are clearly observed when $\omega_{eg} \approx \omega_1$ in Fig. 2(a) and $\omega_{eg} \approx \omega_2$ in Fig. 2(b), respectively. The coupling strengths of $g_3 = 2\pi \times 36$ MHz (corresponding to the interaction $|0e0\rangle <=> |1g0\rangle$ at $\delta\Phi \approx \pm 9 \times 10^{-3}\Phi_0$) and $g_2 = 2\pi \times 78$ MHz ($|0e0\rangle <=> |0g1\rangle$ at $\delta\Phi \approx \pm 19.5 \times 10^{-3}\Phi_0$) are obtained by fitting the anticrossings.

In Fig. 2(c), we use the two-tone microwave spectroscopy technique to find the energy levels of the atom-resonator coupled system [21]. We measure the transmission at a fixed frequency close to ω_1 and sweep the pumping frequency in the range from 1 to 16 GHz (limited by the bandwidth of the entire system). However, we show our theoretical calculations (which are in a good agreement with the experimentally measured lines) above the bandwidth limit by dashed lines. The applied probing power is sufficiently low to keep the average number of photons inside the resonator less than one ($\langle N_1\rangle < 1$). At $\delta\Phi \neq 0$, all the transitions between the three levels are allowed [14]. The black dashed lines in Fig. 2(a), Fig. 2(b), and Fig. 2(c) are the fitting curves obtained from the Hamiltonian of the atom-resonator system [17]. The dashed red box in
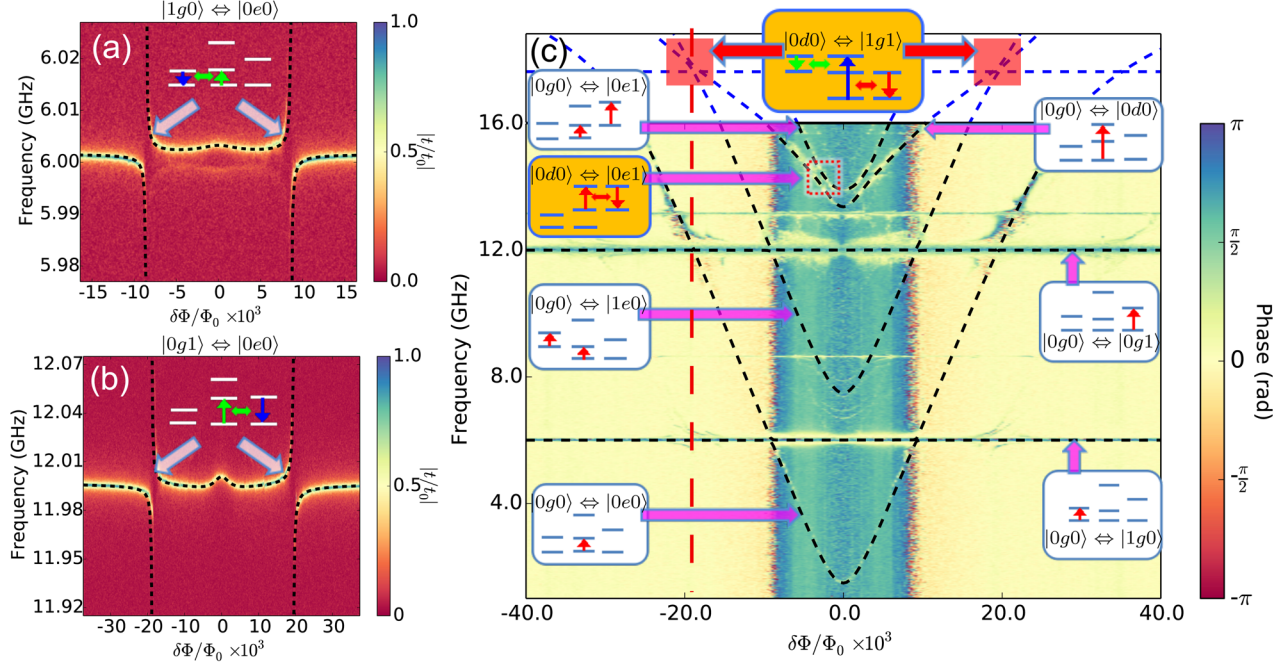
FIG. 2 (color online).   Energy levels of the three-level atom-resonator coupled system. (a), (b) Normalized transmission amplitude through the resonator modes as a function of $\delta\Phi$. The black dashed lines are theoretical fittings from the full system Hamiltonian. (c) Intensity plot of the phase of a transmission signal as a function of driving frequency and $\delta\Phi$. The black dashed lines represent theoretical calculations. Our goal is to study the double resonance shown in Fig. 1(d), which takes place under the conditions marked by the red squares.

Fig. 2(c) shows the avoided crossing due to the inter-action between $|0d0\rangle$ and $|0e1\rangle$ characterized by $g_4 = 2\pi \times 205$ MHz at $\delta\Phi \approx \pm 2.5 \times 10^{-3}\Phi_0$, where the second excited atomic state is converted into a photon in r_2 and the first excited atomic state. Note that g_4 extracted from the experiment is also consistent with the theoretical calculations [18].

To couple the oscillators via the atomic transitions, we set the bias to $\delta\Phi_b = -18 \times 10^{-3}\Phi_0$ (red dashed line), where $\omega_{eg} \approx \omega_2$ and $\omega_{de} \approx \omega_1$, and apply the external microwave drive at a pumping frequency of $\omega_p = 2\pi \times 18.0055$ GHz. Although g_1 cannot be directly measured, we take its value as $2\pi \times 90$ MHz from simulations, which well reproduces other couplings (detailed in the Supplemental Material [18]). Strong emission peaks appear when the pumping power exceeds $P \approx -100$ dBm. The emission disappears, when the atom is detuned from the double resonance. We assume that the threshold has a different nature from conventional lasing and is due to the remaining detuning between ω_{de}, ω_1 and/or ω_{eg}, ω_2, compensated by Rabi splitting, which according to our estimates is $\Omega/2\pi \approx 900$ MHz at ω_{dg}. This is supported by our simulations [18]. Note also that we expect another resonance close (but not equal) to ω_p. However, it does not affect the overall picture because the drive is essentially classical with many photons in the mode. The emission spectra of the coupled system in the vicinity of ω_1 and ω_2 are simultaneously monitored by two spectral analyzers (SAs). We use the techniques developed in

Ref. [22] to eliminate the noise background of the low temperature amplifier by subtracting traces of OFF from ON emission spectra. The results are shown in Fig. 3(a) (black open triangles) and Fig. 3(b) (black open circles). Importantly, the peaks are well fitted by equal width Lorentzian curves with $\Delta\omega_{e1} \approx \Delta\omega_{e2} = 2\pi \times 0.80$ MHz,
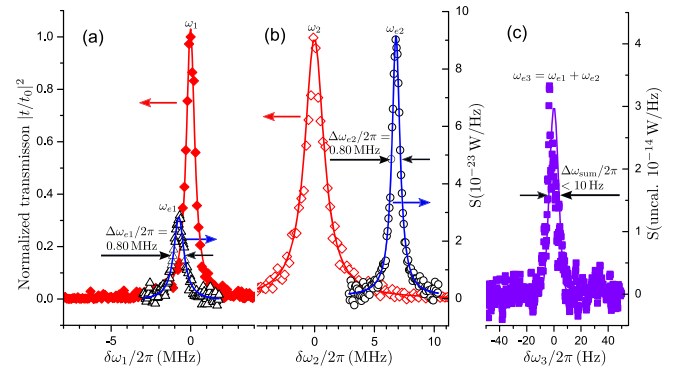

FIG. 3 (color online).   Emission spectra of two-mode CEL and quenching of the phase diffusion noise. (a) and (b) Normalized transmission through oscillators 1 and 2 (red closed and open rhombus) and emission spectra from the oscillators (black open triangulars and circles). The emission spectra have the same widths of $\Delta\omega_{e1} = \Delta\omega_{e2} = 2\pi \times 0.80$ MHz. (c) Quenching of the mutual phase diffusion. The two frequency emissions are amplified and mixed. The resulting up-converted signal (uncalibrated) is very narrow and limited by the SA bandwidth.

indicating the interaction between the oscillators. Note that $\Delta\omega_{e1,2}$ is about two times lower than κ_2 and three times lower than the effective relaxation rate of the entire system of $\kappa_1 + \kappa_2 \approx 2\pi \times 2.57$ MHz. The center frequencies of the two emission spectra of $\omega_{e1} = 2\pi \times 6.00086$ GHz and $\omega_{e2} = 2\pi \times 12.00471$ GHz are somewhat shifted from ω_1 and ω_2 by $\omega_{e1} - \omega_1 = -2\pi \times 0.74$ MHz and $\omega_{e2} - \omega_2 = 2\pi \times 6.81$ MHz, which is probably due to dispersive shifts from the detuning between the artificial atom and the resonator modes [17]. We emphasise that $\omega_{e1} + \omega_{e2} = \omega_p$ holds with high accuracy. Although the emission frequencies slightly depend on other parameters, such as pumping power and frequency, the above equation still holds [18].

The estimated total emission powers, obtained from the extracted area of the emission curves, are $P_1 \approx -134.4$ dBm and $P_2 \approx -129.4$ dBm, with an accuracy of about 3 dBm due to the uncertainty in the calibration of our setup. They roughly correspond to $\langle N_1 \rangle \approx 5$ photons and $\langle N_2 \rangle \approx 2$ photons at r_1 and r_2, respectively. (The photon number is derived using the equation $\langle N_k \rangle = 2P_k/(\hbar\omega_k\kappa_k)$, where $k = \{1, 2\}$ and the prefactor 2 is due to the escape of photons from either end of the resonator with equal probability.) The ratio $\langle N_1 \rangle/\langle N_2 \rangle$ is found to be close to the expected value as the photon creation rate in each mode under stationary conditions is expected to be given by $\langle N_1 \rangle\kappa_1 = \langle N_2 \rangle\kappa_2$, which originates from the energy conservation law: each absorbed photon at ω_p is split into a pair of photons at ω_{e1} and ω_{e2}.

To demonstrate quenching of the phase diffusion in the two-mode CEL, we mix the amplified emission signals at ω_{e1} and ω_{e2} using a conventional microwave mixer. Then, we measure the signal around the sum of the frequencies $\omega_{e1} + \omega_{e2}$ by the SA [18]. Note that the phase diffusion in our case is different from the relative phase diffusion in Refs. [4–6] and we call it mutual phase diffusion. To avoid direct leakage of the pumping tone through our circuit, we filter out high frequencies before mixing and confirm the absence of any outcoming signal at ω_p. Next, we simultaneously monitor the signals at ω_{e2} (ω_{e1}) and $\omega_{e1} + \omega_{e2}$. The result shown in Fig. 3(c) demonstrates a strong narrow sum signal at a frequency of exactly ω_p only when emissions at $\omega_{e1,2}$ occur. Despite mixing a pair of signals of $\Delta\omega_e$ width, the resulting peak width of $\Delta\omega_{\text{sum}} = 2\pi \times 9.4$ Hz is found to be limited by the bandwidth of the SA (10 Hz). We note that the Schawlow-Townes condition for the linewidth is expected to be modified in our system to $\Delta\omega_{\text{ST}} = (\kappa_1 + \kappa_2)/(2N_{\text{tot}})$, which is about 250 kHz for 10 photons. The experimentally measured linewidths of different color emissions satisfy the condition $\kappa_1 + \kappa_2 > \Delta\omega_{e1,2} > \Delta\omega_{\text{ST}}$, which usually takes place for conventional lasers due to additional broadening mechanisms. However, the mutual phase diffusion noise (characterized by $\Delta\omega_{\text{sum}}$) is quenched being at least 4 orders of magnitude lower

than $\Delta\omega_{\text{ST}}$, which can be explained by the theoretical model [18].

To further quantify the correlation between the emissions, we down-convert the emission at ω_{e2} by mixing it with the ω_p tone and select out the difference frequency $\omega_p - \omega_{e2}$. Then, we linearly add the resulting signal to that at ω_{e1} using a linear adder and measure the resulting signal by the SA [18]. The intensity of the observed signal is extracted by fitting with a Lorentzian curve [red curve in Fig. 4(a)] and then is studied as a function of the phase delay introduced in the ω_{e1} emitted signal. As shown in Fig. 4(b), we observe the sinusoidal oscillations of the intensity of the interfering signal as a function of the delay, indicating a strong correlation between the two lasing fields. The interference is additional evidence for the quenching of the mutual phase diffusion.

Finally, we briefly summarize other aspects of the system, consisting of the two oscillators coupled through the transitions of the three-level atom, which can be verified experimentally in the future. The single three-level atom CEL system provides an ideal test bed for studying the nonlinear coupling of light in cavity modes. It was theoretically found that in contrast to two-mode squeezed states by parametric amplifiers [23–27], a bright and arbitrarily high degree squeezed light can be generated inside a cavity by a system of atoms interacting with a two-mode cavity because of the strong atomic nonlinearity [3,28,29]. Moreover, the nonlinear coupling of light in the two cavity modes can lead to two-mode squeezed states [1]. We calculate the time dependence of the sum of the quantum fluctuations of the two lasing fields $(\Delta\hat{u})^2 + (\Delta\hat{v})^2$ based on the experimental parameters and find that it can be smaller than two [30–33], which suggests the possible existence of quantum correlation between the two fields in our sample for the short time after tuning on the pump (details are given in the Supplemental Material [18]).
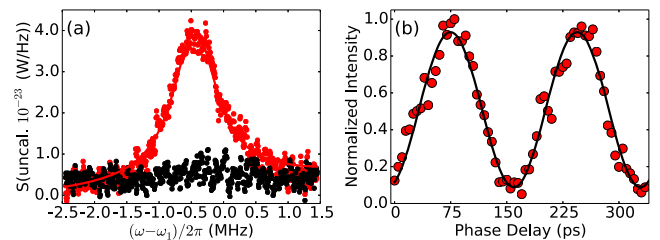

FIG. 4 (color online). Correlation between the two emission modes. (a) Constructive (red dots) and destructive (black dots) interference peaks of the emissions with two different colors. To observe the interference, the ω_{e2} signal is down-converted to $\omega_p - \omega_{e2}$ and a variable delay is introduced in the ω_{e1} emission signal before summing it with $\omega_p - \omega_{e2}$. (b) Interference fringes of the peak amplitudes from (a) as a function of the phase delay between the two signals (red dots). The amplitudes of both signals are adjusted to obtain nearly maximal modulation. The intensity derived from the experimental peaks (red dots) is fitted by a sine function (black curve).

In addition, the quantum coupler provides an ideal (the strongest possible) nonlinearity for weak fields up to the single quantum (photon) level in the strong coupling regime. For example, there is a theoretical discussion about the strong coupling of a phonon mode and a photon mode with a single superconducting three-level artificial atom at single-photon level [34].

In conclusion, we have demonstrated correlated dynamics between two oscillators coupled via transitions of a three-level macroscopic artificial atom. The dynamics is observed as the quantum noise quenching of the mutual phase diffusion in the correlated emission lasing. Our results are the first step to generate the quantum correlation and entanglement between two lasing fields with a single atom, which is an important step towards constructing a quantum network in the microwave domain. This work may also lead to an improvement in ultrahigh-sensitive interferometric measurements [1].

---

[*]zhihui_peng@riken.jp

[†]Oleg.Astafiev@rhul.ac.uk

[1] M. O. Scully and M. S. Zubairy, *Quantum Optics* (Cambridge University Press, Cambridge, England, 1997).

[2] M. O. Scully, Phys. Rev. Lett. **55**, 2802 (1985).

[3] M. O. Scully, K. Wódkiewicz, M. S. Zubairy, J. Bergou, N. Lu, and J. M. ter Vehn , Phys. Rev. Lett. **60**, 1832 (1988).

[4] M. P. Winters, J. L. Hall, and P. E. Toschek, Phys. Rev. Lett. **65**, 3116 (1990).

[5] I. Steiner and P. E. Toschek, Phys. Rev. Lett. **74**, 4639 (1995).

[6] K. Abich and P. E. Toschek, Opt. Commun. **179**, 491 (2000).

[7] A. L. Schawlow and C. H. Townes, Phys. Rev. **112**, 1940 (1958).

[8] J. McKeever, A. Boca, A. D. Boozer, J. R. Buck, and H. J. Kimble, Nature (London) **425**, 268 (2003).

[9] O. Astafiev, K. Inomata, A. O. Niskanen, T. Yamamoto, Y. A. Pashkin, Y. Nakamura, and J. S. Tsai, Nature (London) **449**, 588 (2007).

[10] M. Grajcar, S. H. W. van der Ploeg, A. Izmalkov, E. Il'ichev, H.-G. Meyer, A. Fedorov, A. Shnirman, and G. Schön, Nat. Phys. **4**, 612 (2008).

[11] G. Oelsner, P. Macha, O. V. Astafiev, E. Il'ichev, M. Grajcar, U. Hübner, B. I. Ivanov, P. Neilinger, and H.-G. Meyer, Phys. Rev. Lett. **110**, 053602 (2013).

[12] A. Wallraff, D. I. Schuster, A. Blais, L. Frunzio, R.-S. Huang, J. Majer, S. Kumar, S. M. Girvin, and R. J. Schoelkopf, Nature (London) **431**, 162 (2004).

[13] O. Astafiev, A. M. Zagoskin, A. A. Abdumalikov, Y. A. Pashkin, T. Yamamoto, K. Inomata, Y. Nakamura, and J. S. Tsai, Science **327**, 840 (2010).

[14] Y. X. Liu, J. Q. You, L. F. Wei, C. P. Sun, and F. Nori, Phys. Rev. Lett. **95**, 087001 (2005).

[15] F. G. Paauw, A. Fedorov, C. J. P. M Harmans, and J. E. Mooij, Phys. Rev. Lett. **102**, 090501 (2009).

[16] X. B. Zhu, A. Kemp, S. Saito, and K. Semba, Appl. Phys. Lett. **97**, 102503 (2010).

[17] K. Inomata, T. Yamamoto, P.-M. Billangeon, Y. Nakamura, and J. S. Tsai, Phys. Rev. B **86**, 140508(R) (2012).

[18] See Supplemental Material at http://link.aps.org/supplemental/10.1103/PhysRevLett.115.223603 for single atom two-mode correlated emission lasing theoretical model, experimental methods and details of sample and measurement.

[19] J. E. Mooij, T. P. Orlando, L. Levitov, L. Tian, C. H. van der Wal, and S. Lloy, Science **285**, 1036 (1999).

[20] C. H. van der Wal, A. C. J. ter Haar, F. K. Wilhelm, R. N. Schouten, C. J. P. M. Harmans, T. P. Orlando, S. Lloyd, and J. E. Mooij, Science **290**, 773 (2000).

[21] A. A. Abdumalikov, O. Astafiev, Y. Nakamura, Y. A. Pashkin, and J. S. Tsai, Phys. Rev. B **78**, 180502(R) (2008).

[22] A. A. Abdumalikov, O. V. Astafiev, Y. A. Pashkin, Y. Nakamura, and J. S. Tsai, Phys. Rev. Lett. **107**, 043604 (2011).

[23] G. Milburn and D. F. Walls, Opt. Commun. **39**, 401 (1981).

[24] Z. Y. Ou, S. F. Pereira, H. J. Kimble, and K. C. Peng, Phys. Rev. Lett. **68**, 3663 (1992).

[25] C. Eichler, D. Bozyigit, C. Lang, M. Baur, L. Steffen, J. M. Fink, S. Filipp, and A. Wallraff, Phys. Rev. Lett. **107**, 113601 (2011).

[26] N. Bergeal, F. Schackert, L. Frunzio, and M. H. Devoret, Phys. Rev. Lett. **108**, 123902 (2012).

[27] E. Flurin, N. Roch, F. Mallet, M. H. Devoret, and B. Huard, Phys. Rev. Lett. **109**, 183901 (2012).

[28] J. Gea-Banacloche, N. Lu, L. M. Pedrotti, S. Prasad, M. O. Scully, and K. Wódkiewicz, Phys. Rev. A **41**, 369 (1990).

[29] J. Gea-Banacloche, N. Lu, L. M. Pedrotti, S. Prasad, M. O. Scully, and K. Wódkiewicz, Phys. Rev. A **41**, 381 (1990).

[30] H. Xiong, M. O. Scully, and M. S. Zubairy, Phys. Rev. Lett. **94**, 023601 (2005).

[31] H. T. Tan, S. Y. Zhu, and M. S. Zubairy, Phys. Rev. A **72**, 022305 (2005).

[32] S. Qamar, H. Xiong, and M. S. Zubairy, Phys. Rev. A **75**, 062305 (2007).

[33] L. M. Duan, G. Giedke, J. I. Cirac, and P. Zoller, Phys. Rev. Lett. **84**, 2722 (2000).

[34] Z.-Y. Xue, L.-Na Yang, and J. Zhou, Appl. Phys. Lett. **107**, 023102 (2015).